Stable error-free single channel 160-Gb/s OTDM 100-km transmission via high-precision dispersion management

Nan Jia (贾 楠)[1,2*], Tangjun Li (李唐军)[1,2], Kangping Zhong (钟康平)[1,2], Muguang Wang (王目光)[1,2], Ming Chen (陈 明)[1,2], Dan Lu (卢 丹)[1,2], Wanjing Peng (彭万敬)[1,2], and Jianfeng Chi (池剑锋)[1,2]

[1] *Key Lab of All Optical Networks and Advanced Communication Network of EMC, Beijing Jiaotong University, Beijing 100044, China*

[2] *Institute of Lightwave Technology, Beijing Jiaotong University, Beijing 100044, China*

[*] *E-mail: 08111026@bjtu.edu.cn*

Received January 4, 2010

A single channel with a 160-Gb/s optical time-division-multiplexing (OTDM) transmission over 100 km is fabricated. With the help of 500-GHz optical sampling oscilloscopes, the fiber length is adjusted to the order of 10 m, which corresponds to the accuracy of 0.4 ps for the dispersion compensation. The dispersion map is optimized for the 100-km transmission link. A completely error-free transmission with the power penalty of 3.6 dB is achieved for 2 h without using forward error correction.

OCIS codes: 060.2330, 060.2360, 060.4230, 060.4256, 060.2400.

doi: 10.3788/COL20100808.0741.

The increasing demand for communication networks has led to a serious need for higher transmission capacities. Wavelength-division-multiplexing (WDM) techniques have fulfilled the demand to some extent in recent years, but it will be unable to meet the ever increasing requirement for larger capacity transmission in the future. Optical time-division-multiplexing (OTDM) has been studied for more than a decade as an alternative for increasing the total transmission capacity. In 1993, the first 100-Gb/s OTDM transmission was achieved through a 36-km fiber link[1]. Chromatic dispersion, the most basic characteristic of fiber, is cumulative and increases linearly with transmission distance. More importantly, it increases quadratically with data rate, and the power penalty for uncompensated dispersion increases exponentially with distance[2−4]. In the 160-Gb/s OTDM transmission over 100 km, data transmission is even more strongly affected by chromatic dispersion. Therefore, techniques to compensate for or minimize dispersion are essential for high-capacity transmission. Based on the previous studies[5−7], more effective high-precision dispersion compensation and dispersion management methods are needed to maintain good signal quality and increased system stability. In this letter, we aim to achieve a stable error-free 160-Gb/s OTDM return-to-zero (RZ) transmission over 100 km without forward error correction (FEC) or polarization mode dispersion (PMD) compensation.

For the ultra-short pulse used in a 160-Gb/s OTDM system, both dispersion (D) and dispersion slope ($\mathrm{d}D/\mathrm{d}\lambda$) should be simultaneously compensated. The dispersion slope produces oscillations near the trailing edge of the data pulse, even if $D(\lambda) = 0$ for the center wavelength (λ) of the pulse[8]. In this experiment, a dispersion compensating fiber (DCF) was adopted because it was the most widely used technique to compensate for dispersion. The nonlinear Schrödinger equation accounted for the dispersive effects by including β_2 and β_3. It negated the nonlinear effects as follows[9]:

$$\mathrm{i}\frac{\partial U}{\partial z} = \frac{\beta_2}{2}\frac{\partial^2 U}{\partial T^2} + \mathrm{i}\frac{\beta_3}{6}\frac{\partial^3 U}{\partial T^3}. \tag{1}$$

By solving Eq. (1), the transmitted field is obtained from

$$U(z,T) = \frac{1}{2\pi}\int_{-\infty}^{\infty}\widetilde{U}(0,\omega) \exp\left[\frac{\mathrm{i}}{2}\beta_2\omega^2 z + \frac{\mathrm{i}}{6}\beta_3\omega^3 z - \mathrm{i}\omega T\right]\mathrm{d}\omega, \tag{2}$$

where $\widetilde{U}(0,\ \omega)$ is the Fourier transform of the incident field at $z = 0$. For a dispersion map consisting of two fiber segments, Eq. (2) becomes

$$U(L,T) = \frac{1}{2\pi}\int_{-\infty}^{\infty}\widetilde{U}(0,\omega)\exp\left[\frac{\mathrm{i}}{2}\omega^2(\beta_{21}L_1 + \beta_{22}L_2) + \frac{\mathrm{i}}{6}\omega^3(\beta_{31}L_1 + \beta_{32}L_2) - \mathrm{i}\omega T\right]\mathrm{d}\omega. \tag{3}$$

For fiber links containing a single-mode fiber (SMF) and DCF, with lengths of L_{SMF} and L_{DCF}, the conditions for broadband dispersion compensation are given by:

$$\begin{aligned}\beta_{2\mathrm{SMF}}L_{\mathrm{SMF}} + \beta_{2\mathrm{DCF}}L_{\mathrm{DCF}} = 0,\\ \beta_{3\mathrm{SMF}}L_{\mathrm{SMF}} + \beta_{3\mathrm{DCF}}L_{\mathrm{DCF}} = 0,\end{aligned} \tag{4}$$

where β_{2j} and β_{3j} are the group velocity dispersion (GVD) and the third-order dispersion (TOD) parameters for SMF and DCF (j = SMF, DCF), respectively.

Dispersions for DCF and SMF were measured using CD400 (PE. fiberoptics Ltd., UK). At 1554.3 nm, the dispersion values for DCF and SMF are –145.64 and 16.63 ps/(nm·km), respectively (Fig. 1). Then, the total 100.11-km fiber link was measured. Results (Fig. 2) indicate that the center ripple of the bandwidth is less than 2 ps, and the residual dispersion is less than 1 ps/nm at the distal end of the transmission link. In addition, the

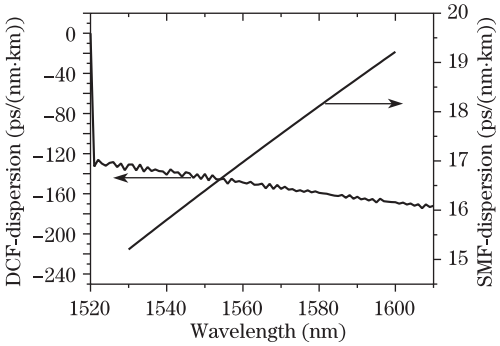

Fig. 1. Measured dispersion values for DCF and SMF.

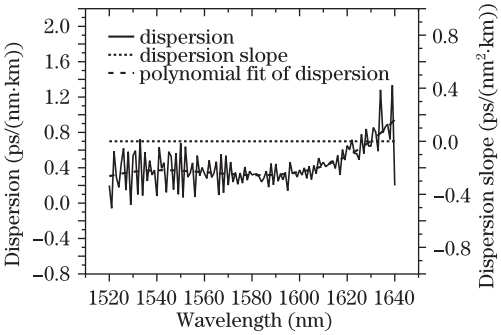

Fig. 2. Measured dispersion and dispersion slope values for fiber over a 100.11-km transmission (89.79 km SMF+10.32 km DCF).

accuracy of CD400 is insufficient when the dispersion value reaches zero. Results in Fig. 2 can quantitatively compensate for the dispersion. Moreover, the PMD coefficient of SMF is less than 0.05 $(\text{ps/km})^{\frac{1}{2}}$, and the PMD of DCF is 0.29 ps. Hence, the total PMD of the transmission link is less than 0.76 ps, which also contributes to pulse broadening. In this experiment, the 10-m level was accurately fine-tuned to compensate for both dispersion and dispersion slope. Furthermore, results demonstrate that the net residual dispersion is within the tolerance limits for this system.

The transmission link consists of three spans of fiber, corresponding to three positions of the DCF (the front,

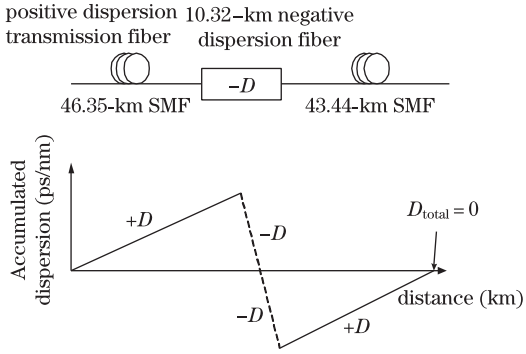

Fig. 3. Dispersion map for SMF paired with DCF.

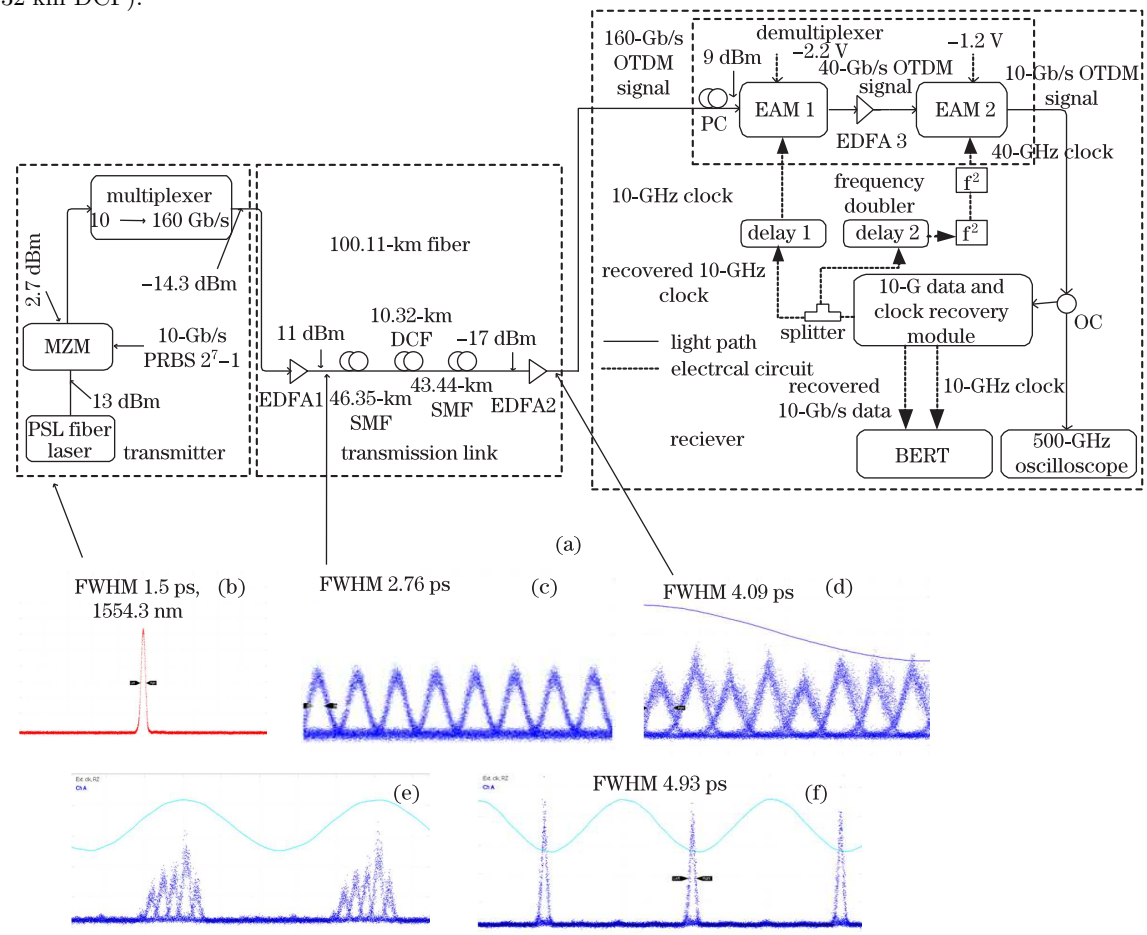

Fig. 4. (a) Experimental setup of 160-Gb/s OTDM transmission over 100-km fiber, (b) waveform of 10-GHz signal, (c) eye diagram of multiplexed 160-Gb/s signal, (d) eye diagram of 160-Gb/s signal after 100-km transmission, (e) eye diagram of the data signal after EAM1, (f) eye diagram of de-multiplexed 10-Gb/s signal. Eye diagrams were measured using a 500-GHz OSO provided by EXFO.

the middle, or the end of the fiber link). The middle position was chosen as the optimal place for DCF for the following reasons: DCF has high loss, so a gain stage is required for the DCF module to avoid excessively low signal levels; DCF has a cross-section that is four times smaller than that of SMF, so a higher nonlinearity, such as self-phase modulation, limits the maximum launch power into a DCF module[10]. Placing the DCF after the 46.35-km SMF ensured that the optical power into the DCF module would not induce excessive nonlinear effects. The DCF was not placed at the end of the fiber link because β_2 was large locally but nearly vanished on average in this pseudo-linear transmission system. The pulse developed an oscillating tail because of TOD and exhibited spectral narrowing if the DCF was placed after the SMF[9]. Then, the erbium-doped fiber amplifier (EDFA2) stage amplifies the dispersion-compensated signal to a power level suitable for launching in the electronic absorption modulator (EAM1). The optimized dispersion map, which suppresses the nonlinearity together with the appropriate power input, is shown in Fig. 3. All fibers used in the transmission link were fabricated by Yangtze Optical Fiber and Cable Co. (YOFC).

Figure 4(a) schematically shows the experimental setup. It consists of a transmitter, a transmission link, and a receiver. The 160-Gb/s transmitter is comprised of a 10-GHz picosecond-pulsed fiber laser (PSL-10-1T, Calmar Optcom Model) that produces an optical pulse train at repetition rates of 10 Gb/s (sech^2 pulses, full-width at half-maximum (FWHM) 1.5 ps, λ = 1554.3 nm). The corresponding wave pattern is shown in Fig. 4(b). The 10-GHz pulse train was launched into an external $LiNbO_3$ Mach-Zehnder modulator (MZM) driven by a psuedo-random bit sequence (PRBS) pattern generator (Agilent N4901B, 2^7–1). A fiber delay line multiplexer provided a 160-Gb/s data signal at the input of the fiber link.

The transmission link consists of three parts: two spans of SMFs measuring 46.35 and 43.44 km, respectively (total length = 89.79 km), and a span of DCF measuring 10.32 km. The multiplexers are homemade and have excellent temperature stability, high-time delay accuracy, and polarization insensitivity. The accuracy of the pulse delay time was < 50 fs (Fig. 4(c)). The 160-Gb/s RZ data signal was then amplified by EDFA1 to 11 dBm and then fed into the transmission link with a total insertion loss of 28 dB, including all splices and connectors. The measured pulse width was 2.76 ps, which was 1.26 ps greater than that of the picosecond laser (PSL). The increase was caused by the combined fiber length of the optical jumper wire and the four-stage multiplexer in the transmitter dash box (~30 m). After the transmission was amplified by EDFA2, the eye diagram of the 160-Gb/s data signal was measured (Fig. 4(d)). The pulse width after launching (4.09 ps) was 1.33 ps wider than that before launching. This result confirms that an optimal dispersion management is achieved in the transmission link, and it is 2.59 ps wider than the original pulse width after the 100.02-km transmission. In Fig. 4(d), the pedestal of the pulse slightly overlaps with the border of the tolerance limits for system dispersion. It has no significant effect on the system. In addition to the inherent measurement error of the 500-GHz optical

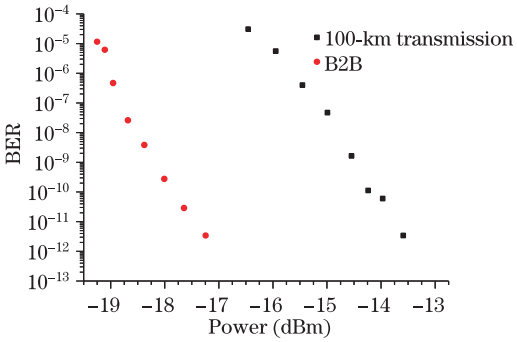

Fig. 5. BER measurements of 160-to-10 Gb/s.

sampling oscilloscope (OSO), the fiber (~10 m) connected from the measure points to the OSO also broadens the pulse width. Therefore, the actual pulse width is narrower than the measured one.

The data receiver is comprised of a pair of concatenated EAMs combined with a 10-GHz clock recovery module. It is based on a phase-locked loop (PLL), which is used to implement de-multiplexing and clock recovery simultaneously for 160-Gb/s OTDM signals. The clock derived from the de-multiplexed signal by the clock recovery module subsequently worked as a driven signal to control the EAMs of generating temporal optical sampling windows, which were biased at –2.2 and –1.2 V. By gradually adjusting the phase shift of the extracted clock, the signal could be de-multiplexed with high quality. A polarization controller (PC) was placed before EAM1 (driven at 10 GHz) to adjust the polarization state of the input signal. There was no PC before EAM2 (driven at 40 GHz) because it was polarization-independent. EDFA3 was applied to compensate for the relatively larger insertion losses in the EAMs. Then, the de-multiplexed 10-Gb/s signal was divided into two parts: one was monitored by a 500-GHz OSO (PSO-100 provided by EXFO); the other was injected to the clock recovery module. Furthermore, this de-multiplexed structure provides stability and easy control and enables extinction-ratio regeneration. By finely tuning the variable electrical delay line and the bias of the EAM1 and EAM2, an error-free de-multiplexing is achieved. The eye diagram of the signals after EAM1 is shown in Fig. 4(e). In Fig. 4(f), the eye diagram of the de-multiplexed 10-Gb/s signals is clear and open, and the non-target channel is sufficiently suppressed.

Figure 5 shows the bit error rate (BER) and back-to-back (B2B) plot against the received power for the system. After transmission, the received sensitivity (BER = 10^{-12}) is 13.13 dBm, which corresponds to a B2B sensitivity of 16.75 dBm. The power penalty (~3.6 dB) is caused by the amplified spontaneous emission (ASE) noise of the EDFA and the de-multiplexing of the two EAMs. The error-free (BER = 10^{-12}) transmission states lasted for 2 h without re-adjustment. The stable error-free transmission can be attributed to the homemade multiplexer with excellent temperature stability and polarization insensitivity, accurate dispersion compensation and optimized dispersion management (the decisive factor), power optimization, and the optimized switching window generated by two concatenate EAMs. Precise adjustments were made using the 500-GHz OSO, making the system more robust against degradation. Be-

cause the setup did not include automatic feedback comparison from a commercial system, errors occur after 2 h. The errors are caused by ASE noise from the homemade EDFA, slow drift of the fourth pulse multiplexer, etc. Results indicate that 160-Gb/s RZ transmission over 100 km can be achieved by accurate dispersion management, and error-free operation can be prolonged using FEC.

In conclusion, the stable error-free 160-Gb/s OTDM system transmission over 100 km is achieved via high-precision dispersion management. Moreover, the stable PSL, the home-made multiplexer, the optical gate, and the clock recovery enable error-free operation for 2 h. Operation is only limited by slow drifting effects in the laboratory system due to the absence of an automatic feedback. No BER is measured without re-adjustment and without FEC or PMD-compensation, the use of which will further improve the system margin. These results have demonstrated that data rates of 160 Gb/s per channel can be achieved for stable error-free RZ transmission through precision dispersion management.

This work was supported by the Natural Science Foundation of Beijing (No. 4062027), the National "863" Project of China (Nos. 2007AA01Z258 and 2008AA01Z15), and the National Natural Science Foundation of China (Nos. 60877042 and 60837003).

References

1. S. Kawanishi, H. Takara, and K. Uchiyamaetal, in *Proc. eedings of ECOC'93* 3 (1993).
2. I. Kaminow and T. Li, (eds.) *Optical Fiber Telecommunications IV B* (Academic Press, San Diego, 2002) p.645.
3. A. Bogoni, L. Potì, P. Ghelfi, M. Scaffardi, C. Porzi, F. Ponzini, G. Meloni, G. Berrettini, A. Malacarne, and G. Prati, Opt. Fiber Technol. **13,** 1 (2007).
4. L. Pei, T. Ning, C. Qi , Y. Ruan, and S. Jian, Chinese J. Laser (in Chinese) **37,** 142 (2010).
5. T. Gong, F. Yan, D. Lu, M. Chen, P. Liu, P. Tao, M. Wang, T. Li, and S. Jian, Opt. Commun. **282,** 3460 (2009).
6. M. Chen, D. Lu, T. Gong, B. Lv, M. Wang, T. Li, and S. Jian, Chin. Phys. Lett. **26,** 074211 (2009).
7. B. Lv, T. Gong, O. Xu, S. Lu, F. Zhang, X. Qin, J. Cao, M. Wang, J. Zhang, and S. Jian, Acta Opt. Sin. (in Chinese) **28,** 1434 (2008).
8. H. Weber, R. Ludwig, S. Ferber, C. Schmidt-Langhorst, M. Kroh, V. Marembert, C. Boerner, and C. Schubert, J. Lightwave Technol. **24,** 4616 (2006).
9. G. P. Agrawal, *Nonlinear Fiber Optics* (4th edn.) (Academic Press, San Diego, 2009).
10. I. P. Kaminow, T. Li, and A. E. Willner, *Optical Fiber Telecommunications V B* (Academic Press, San Diego, 2008).